

Padé Approximation and Partition Function Zeros

R. G. M. Rodrigues^a

^a*Instituto de Computação, Universidade Estadual de Campinas (UNICAMP), Av. Albert Einstein, 1251, Campinas, 13083-852, São Paulo, Brazil*

Abstract

Fisher zeros play a central role in the theoretical understanding of phase transitions. However, their computation requires knowledge of the density of states, which limits their practical applicability. Alternative approaches based on the Energy Probability Distribution (EPD) and Moment Generating Function (MGF) alleviate the computational cost but suffer from convergence issues in the two-dimensional **anisotropic Heisenberg** model (XY model). In this work, we introduce a Padé approximation to systematically reduces the number of zeros required in the Fisher, EPD, and MGF formulations without loss of accuracy. Moreover, since the Fisher zeros formulation does not rely on a convergence algorithm, their combination with a Padé approximation enables a reliable analysis of the XY model while significantly reducing computational cost. Applications to the two-dimensional Ising and XY models demonstrate substantial reductions in polynomial degree and computation time while preserving accurate estimates of the critical temperature.

Keywords: Phase transitions, Fisher zeros, Energy Probability Distribution zeros, Moment Generating Function zeros, Padé approximation

1. Introduction

The characterization of phase transitions as non-analyticities of the free energy admits an elegant formulation in terms of partition function zeros. Yang and Lee [1, 2] established a rigorous link between non-analytic behavior in the free energy and the complex zeros of the partition function. By analytically continuing the fugacity into the complex plane, they showed that the zeros condense into loci that may pinch the real axis in the thermodynamic limit; such pinch points signal the onset of non-analytic behavior and thus identify phase transitions. The zeros closest to the real axis govern the singular behavior of the free energy and are referred to as dominant zeros. This framework has been extensively applied to investigate critical phenomena in diverse physical systems [3, 4, 5, 6, 7] and has also been found in experimental settings [8, 9]. Fisher later extended this approach to the canonical ensemble by analytically continuing the temperature into the complex domain [10].

While the Fisher zeros provides a rigorous foundation for the study of phase transitions, its computational implementation faces significant challenges. The method depends on the explicit knowledge of the density of states, which is often difficult to determine, and requires the solution of a high degree polynomial, whose coefficients derived from the density of states and can span many orders of magnitude. To overcome these difficulties, alternative formulations such as the Energy Probability Distribution (EPD) zeros [11], the Moment Generating Function (MGF) zeros [12], and the cumulant method [13] have been proposed. These methods exploit information contained in the energy probability distribution (EPD), energy moments (MGF) or energy cumulants (cumulants method) to infer the critical temperature.

All of these quantities are considerably easier to obtain than the density of states. Since each method relies on partial statistical information about the system, an iterative refinement algorithm is employed to ensure convergence toward the true critical temperature. These approaches have demonstrated high accuracy and robustness in the analysis of discontinuous, continuous and topological phase transitions [11, 12, 14, 15, 13].

Compared with the Fisher zeros, the EPD and MGF zeros approaches yield a smaller number of zeros in the complex plane and involve polynomials that are easier to handle numerically. In this work, a Padé approximation is employed to further reduce the number of zeros required in all these formulations while preserving their accuracy. The method can also be applied directly to the Fisher zeros, effectively decreasing the number of roots to be determined, although it still requires knowledge of the density of states. The approach is validated for the two-dimensional Ising and XY models.

The application of zeros based methods to the two-dimensional XY model presents fundamental challenges. In contrast to the Ising case, the XY model does not exhibit a well defined dominant zero. Instead, the transition is encoded in a cusp formed by the accumulation of zeros in the complex plane [16]. As a consequence, the convergence algorithms of the EPD and MGF formulations become unreliable, and their local reconstruction of the zeros distribution prevents the identification of the cusp. In the following sections, we show that these limitations can be overcome by combining the Fisher zeros formulation with a Padé approximation, which enables a reliable analysis of the XY model while retaining a reduced number of zeros.

This paper is organized as follows. Sections 2, 3, and 4 provide brief

reviews of the Fisher, EPD, and MGF zeros methods, respectively, while the Padé approximation is introduced in Section 5. The Ising and XY models are described in Sections 6 and 7. Sections 8.1, 8.2, and 8.3 then present the application of the Padé approximation to the Fisher, EPD, and MGF zeros. Section 8.4 discusses the limitations of the EPD and MGF approaches in the analysis of the XY model, and Section 8.5 reports the final results for both the XY and Ising models.

2. Fisher Zeros

The concept of Fisher zeros [10] constitutes an extension of the Yang–Lee theory to the canonical ensemble. Whereas the Yang–Lee zeros originate from the analytic continuation of the fugacity into the complex plane, Fisher’s formulation extends the inverse temperature, $\beta = 1/(k_B T)$, to complex values. In this framework, the canonical partition function can be expressed as

$$Z = \sum_E g(E) e^{-\beta E} = e^{-\beta \varepsilon_0} \sum_n g_n z^n, \quad (1)$$

where $z = e^{-\beta \varepsilon}$, k_B is the Boltzmann constant, and $g(E)$ denotes the density of states. The energy spectrum is discretized as $E_n = \varepsilon_0 + n\varepsilon$, with ε_0 the ground state energy, ε the energy bin, and $g_n = g(E_n)$ the corresponding density of states value [16]. This polynomial has complex conjugate roots and, since $g(E) \geq 0$, any real root must be negative. A real positive root appear only in the thermodynamic limit, as the dominant zero approaches the positive real axis, signaling the point at which the free energy develops a non-analyticity and a phase transition occurs.

For finite systems, the partition function remains analytic, and the dominant zero does not lie on the real axis but rather in its close vicinity. Its real

part, however, provides an estimate of the pseudo-critical temperature $T_c(L)$ for a finite lattice of size L . Through standard finite-size scaling analysis, one can then extrapolate $T_c(L)$ to the thermodynamic limit obtaining the an estimative for the critical temperature T_c .

3. The Energy Probability Distribution Zeros

The Energy Probability Distribution zeros method [11] provides an alternative formulation to the Fisher zeros, obtained by rescaling the z variable and expressing the partition function in terms of the energy probability distribution. This reformulation allows the zeros to be determined from a histogram rather than from the density of states, thus simplifying the numerical implementation while preserving the underlying analytical structure.

The EPD polynomial is found multiplying Eq. 1 by the identity $e^{-\beta_0 E} e^{\beta_0 E} = 1$, which yields

$$Z = \sum_E g(E) e^{-\beta_0 E} e^{-\Delta\beta E} = e^{-\Delta\beta\varepsilon_0} \sum_n h_{\beta_0}(n) x^n, \quad (2)$$

where $\beta_0 = 1/(k_B T_0)$ is an arbitrary reference inverse temperature, $\Delta\beta = \beta - \beta_0$, and $x = e^{-\Delta\beta\varepsilon}$. The coefficients $h_{\beta_0}(n) = g_n e^{-\beta_0 E_n}$ correspond to the non-normalized energy probability distribution evaluated at β_0 .

Since these coefficients form a probability distribution, one can safely introduce a cutoff threshold h_t and discard coefficients with probabilities below it without affecting the zeros relevant to the thermodynamics at β_0 . This truncation effectively reduces the polynomial degree and, consequently, the computational cost, while retaining all physically meaningful zeros. In the limit where no cutoff is applied and all states are retained, the full distribution of Fisher zeros is naturally recovered.

Because the EPD zeros are a rescaled form of the Fisher zeros through the transformation $x = z/e^{-\beta_0\varepsilon}$, the Fisher dominant zero $z_c = e^{-\beta_c\varepsilon}$ maps onto $x = 1$ when $\beta_0 = \beta_c$. This property enables the construction of an iterative algorithm that systematically refines an initial arbitrary $\beta_0(L)$ towards $\beta_c(L)$. The algorithm is given by:

1. Build a single histogram $h_{\beta_0}^j$ at β_0^j and rescale it so that $\max(h_{\beta_0}^j(n)) = 1$.
2. Find the zeros of the polynomial with coefficients given by $h_{\beta_0}^j$.
3. Discard the coefficients $h_{\beta_0}^j(n)$ that are smaller than a chosen threshold h_t .
4. Find the dominant zero, x_c^j .
 - (a) If x_c^j is close enough to the point $(1, 0)$, stop.
 - (b) Else, make

$$\beta_0^{j+1} = -\frac{\ln(\Re e\{x_c^j\})}{\varepsilon} + \beta_0^j$$

and go back to 1.

4. Moment Generating Function Zeros

The moment-generating function zeros [12] are obtained by expanding the exponential term in the EPD polynomial, Eq. 2, as a power series and exchanging the order of summation. Through this expansion, the polynomial coefficients become the moments of the energy probability distribution evaluated at β_0 . The canonical partition function can thus be expressed as

$$Z(\beta) = Z(\beta_o) \sum_{k=0}^{\infty} \frac{m_k(\beta_o)}{k!} y^k, \quad (3)$$

where $Z(\beta_o)$ is a constant, $y = -\Delta\beta$ and $m_k(\beta_o) = \langle E^k \rangle_{\beta_o}$ are the moments of the energy. Since $Z(\beta_o)$ is only a constant, the zeros of the canonical partition function and the zeros of the MGF contain the same information.

The main advantage of this method over the EPD zeros approach is that the polynomial degree can be reduced by truncating the series at a finite order k_{\max} , rather than by introducing an arbitrary discard threshold. Furthermore, since this formulation depends solely on the energy moments, it does not impose a discretization of the energy spectra eliminating arbitrary parameters such as the energy bin ε .

The EPD zeros and MGF zeros are connected through the transformation $x = e^{y\varepsilon}$ allowing properties of the EPD zeros to be directly extended to the MGF formulation. For example, since the EPD dominant zero is at $x_c = 1$ for $\beta_o = \beta_c$, the MGF dominant zero must be at the origin, $(0, 0)$, for $\beta_o = \beta_c$. Moreover, the convergence algorithm originally developed for the EPD zeros can be readily adapted to the MGF case. The following modified procedure can be employed to estimate $\beta_c(L)$, assuming a truncation at a sufficiently order k_{\max} ,

- 1 Find the energy moments $m_k(\beta_o) = \langle E^k \rangle$ at $\beta_o^j(L)$.
- 2 Find the zeros of the polynomial with coefficients given by $m_k(\beta_o^j)/k!$.
- 3 Find the dominant zero, $y_c^j(L)$.
 - a) If y_c^j is close enough to the point $(0, 0)$, stop.
 - b) Else, make $\beta_o^{j+1}(L) = \beta_o^j(L) - \Re\{y_c^j(L)\}$ and go back to 1..

5. Padé Approximation

Inspired by the MGF approach, which estimates the zeros through a truncated Taylor expansion, we employ a Padé approximation to represent the partition function. This technique expresses a function as a ratio of two polynomials, providing a rational approximation that generally exhibits superior convergence properties compared to a truncated Taylor series. Moreover, the Padé expansion can be straightforwardly applied to any of the previously discussed methods.

In order to construct the Padé approximation, consider a function f represented by a power series,

$$f(x) = \sum_{k=0}^K a_k x^k, \quad (4)$$

the Padé approximant of order $[m/n]$ is defined as

$$F_{m,n}(x) = \frac{P_m(x)}{Q_n(x)} = \frac{\sum_{i=0}^m p_i x^i}{1 + \sum_{j=1}^n q_j x^j}, \quad (5)$$

where the coefficients $\{p_i\}$ and $\{q_j\}$ are determined such that the Taylor expansion of $F_{m,n}(x)$ agrees with $f(x)$ up to the highest possible order, i.e.,

$$f(x) - F_{m,n}(x) = \mathcal{O}(x^{m+n+1}), \quad (6)$$

where $(m+n+1) \leq K$. Detailed derivations of the procedure used to determine the coefficients p_i and q_j required to construct the Padé approximant are can be found in [17]. For the present discussion, it suffices to say that the coefficients p_i and q_j are fully determined once the set a_k is known.

The main idea is to apply a Padé approximation in each of the previously introduced methods, where the coefficients a_k correspond to different physical

quantities depending on the formulation: the density of states in the Fisher method, the energy probability distribution in the EPD, and the energy moments in the MGF. By truncating the Padé approximation through an appropriate choice of m and n , the order of the polynomial that must be determined is reduced, thereby simplifying the approach.

The resulting polynomials $P_m(x)$ and $Q_n(x)$ have distinct interpretations. The zeros of $P_m(x)$ correspond to the zeros of interest such as the Fisher, EPD, or MGF, while the zeros of $Q_n(x)$ signal the presence of spurious poles, marking regions where the Padé approximation loses reliability. Consequently, the number of zeros captured by the Padé construction is controlled by the choice of the polynomial orders m and n . In particular, the parameter m sets the number of partition function zeros, and in the asymptotic regime of large m and small n , the full set of zeros is recovered. This flexibility enables the selective reconstruction of a subset of zeros while preserving the overall accuracy of the approximation. A detailed analysis of the respective effects of m and n is presented in Sec. 8.

5.1. Shifted Padé Approximation

In practical applications, the quality of a series expansion can be significantly improved by centering the expansion around a point of interest, rather than the origin. In particular, when the relevant physical information is concentrated near a specific complex value z_0 (for instance, close to a leading zero of the partition function), it is advantageous to first shift the expansion variable and then apply the Padé procedure.

Consider a generic truncated power series representation of a function f ,

$$f(z) = \sum_{n=0}^N b_n z^n, \quad (7)$$

where the coefficients b_n are known from one of the formulations discussed previously (e.g., Fisher zeros, EPD, or MGF). We rewrite this polynomial as an expansion around a shifted point z_0 by introducing the variable $w = z - z_0$.

Using the binomial expansion, the series can be expressed as

$$f(z) = \sum_{k=0}^N c_k w^k, \quad (8)$$

with coefficients

$$c_k = \sum_{n=k}^N b_n \binom{n}{k} z_0^{n-k}, \quad k = 0, 1, \dots, N. \quad (9)$$

Once the shifted coefficients $\{c_k\}$ are obtained, we construct a Padé approximant of order $[m/n]$ in the variable w . The interpretation given before for the resulting polynomials P_m and Q_n remains unchanged.

Although this strategy can, in principle, be applied to the MGF and EPD zeros, its practical usefulness is limited by the difficulty of predicting the location of the dominant zero during the convergence process. A reliable estimate is only available at the transition temperature, where the dominant zero is expected to lie close to the origin for the MGF formulation and near the point $(1, 0)$ for the EPD formulation. For this reason, in the following sections we restrict the application of the shifted Padé approximation to the Fisher zeros.

This shifted construction offers a significant advantage when applied to the Fisher zeros method. If an approximate location of the dominant zero is

known a priori, the series expansion can be centered near this point, drastically reducing the polynomial order necessary to find the dominant zero. However, a naive implementation of the algorithm used to compute the coefficients c_k would make the method slower than all previously presented approaches, see [Appendix B](#) for details.

6. Ising Model

The two-dimensional Ising model was selected as a test system due to the availability of its exact density of states, which can be computed numerically [\[18\]](#). The model is on a square lattice, where each site i has a spin variable $\sigma_i \pm 1$, and the interaction between nearest neighbors is governed by the Hamiltonian,

$$H = -J \sum_{\langle i,j \rangle} \sigma_i \sigma_j, \quad (10)$$

where J is a coupling constant and the summation runs over all pairs of nearest neighbors. The model exhibits a second order phase transition at the exact critical temperature $T_c = 2/\ln(1 + \sqrt{2})J/k_B$. This model serves as a benchmark for validating the accuracy between the methods presented in this work. Throughout this study, the constants are fixed as $J = 1$ and $k_B = 1$.

7. Anisotropic Heisenberg or XY Model

The two-dimensional **anisotropic Heisenberg** model provides a paradigmatic example of a system undergoing a Berezinskii–Kosterlitz–Thouless (BKT) transition [\[19, 20\]](#), which has been the subject of sustained theoretical and experimental interest for more than four decades [\[21\]](#). Unlike

conventional first- or second-order phase transitions, the BKT transition is topological in nature and does not involve spontaneous symmetry breaking or the emergence of true long-range order [22]. Instead, the low-temperature phase is characterized by quasi-long-range order, with two point correlation functions exhibiting an algebraic decay for $T \leq T_{\text{BKT}}$, while above the transition temperature the correlations decay exponentially.

The transition occurs at a characteristic temperature T_{BKT} , below which the system exhibits a line of critical points extending down to zero temperature. All derivatives of the free energy remain finite at the transition, and for this reason the BKT transition is classified as an infinite order phase transition. Despite the absence of divergences, the free energy is non-analytic for $T \leq T_{\text{BKT}}$ and, in the termodanymic limit, it is spected to see a line of zeros in the Fisher zeros map in the real temperature axis, while for $T > T_{\text{BKT}}$ the zeros should not touch the real positive axis.

To establish notation and provide the basis for the numerical analysis that follows, the XY model is described by the Hamiltonian

$$\mathcal{H} = -J \sum_{\langle i,j \rangle} (S_i^x S_j^x + S_i^y S_j^y), \quad (11)$$

where the summation runs over all nearest-neighbor pairs, $J = 1$ is the coupling constant, and $\mathbf{S}_i = (S_i^x, S_i^y, S_i^z)$ is the spin orientation at site i . Because it shares the same Hamiltonian as the planar-rotator model, whose spins are restricted to two components, the XY model is often confused with it in the literature [23, 24].

8. Results

To investigate the effect of the Padé parameters m and n on each of the methods introduced, we first consider the two-dimensional Ising model with lattice size of $L = 24$. For this model, the exact density of states is known for arbitrary system sizes [18]. This allows a direct determination of the Fisher zeros and provides a benchmark for assessing the accuracy of the Padé approximation. Once validated for this case, the Padé based approach is subsequently applied to estimate the critical temperature of both the Ising and XY models, and the results are compared with those obtained from the original formulations.

For the XY model, the density of states was obtained using a Wang–Landau simulation. Details can be found in [16], and the raw data are available in [25].

8.1. Fisher Zeros

To obtain the Padé approximation for the Fisher zeros, the coefficients a_k in Eq. 4 are taken as the density of states. From these coefficients, the Padé polynomials $P_m(x)$ and $Q_n(x)$ are constructed, where the polynomial orders are determined by the chosen values of m and n . The effect of these parameters on the zeros’ distribution is illustrated in Fig. 1a, which shows the results for $m = [20, 40, 150]$ and $n = 20$. As m increases, the Fisher zeros are gradually restored, approaching the complete distribution obtained from the original formulation.

As shown in Fig. 1b, $m = 150$ is sufficient to accurately identify the dominant zero. It is worth noting that some roots of $Q_n(x)$ coincide with

roots of $P_m(x)$, such overlapping roots should not be considered, as they correspond to regions where the Padé approximation becomes unreliable. This procedure accurately locates the dominant zero using a polynomial of degree 150, representing a reduction to one quarter of the original polynomial order required for the full Fisher zeros map. Furthermore, with the shifted version of the Padé approximation (SPadé), it was necessary only $m = 30$ to find the dominant zero as can be seen in Fig. 2.

8.2. EPD Zeros

The same procedure to construct P_m and Q_n was applied for the EPD zeros, with the only modification being the use of the energy probability distribution as a_k instead of the density of states. Surprisingly, in the case of the EPD zeros this approach does not provide any advantage. The value of m required to obtain a reliable approximation of the dominant zero is nearly identical to the polynomial order used in the standard EPD method, making the Padé approximation effectively redundant. Fig. 3 shows the distribution of zeros for $m = [60, 130]$ and $n = 2$, only for $m = 130$ the dominant zero is correctly estimated, whereas the original EPD polynomial has degree 136. Besides that, a cluster of zeros of Q_n consistently appears near the dominant zero, potentially affecting the precision of its estimation.

8.3. MGF Zeros

While the Padé approximation offers no improvement for the EPD zeros, it significantly reduces the number of zeros required in the MGF method. Fig. 4 illustrates the Padé approximation constructed with half the polynomial degree used in the original MGF formulation. It is noteworthy that the

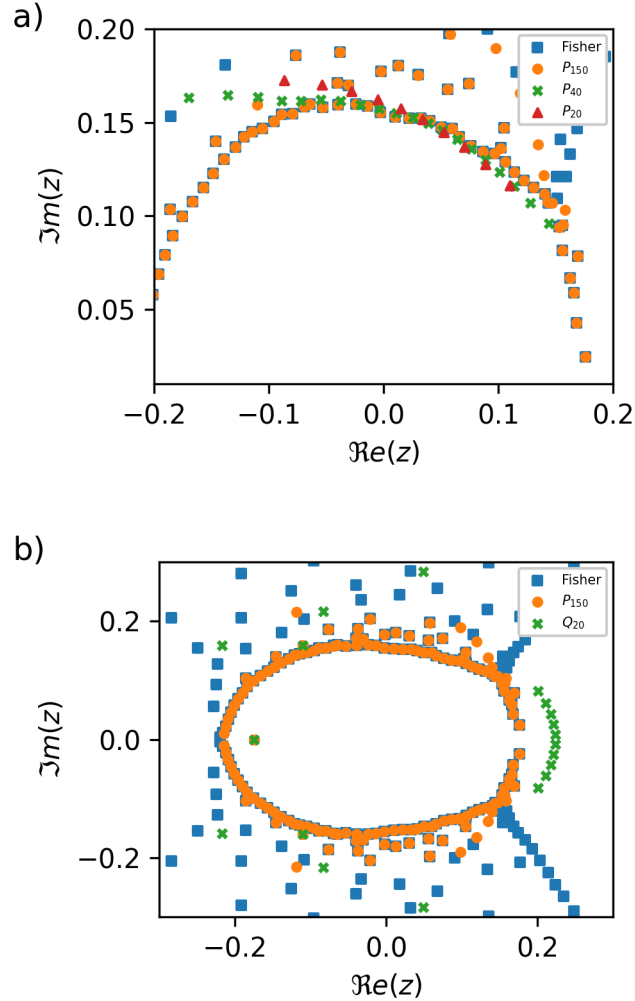


Figure 1: a) Fisher zeros from the Padé approximation with $m = [20, 40, 150]$ and $n = 20$, showing convergence toward the full zero distribution as m increases. b) For $m = 150$, the dominant zero is accurately captured, while overlapping roots of $P_{150}(x)$ and $Q_{20}(x)$ are excluded as invalid points.

parameter m could be further reduced without affecting accuracy. However, we chose m to be half the polynomial degree of the original MGF formulation,

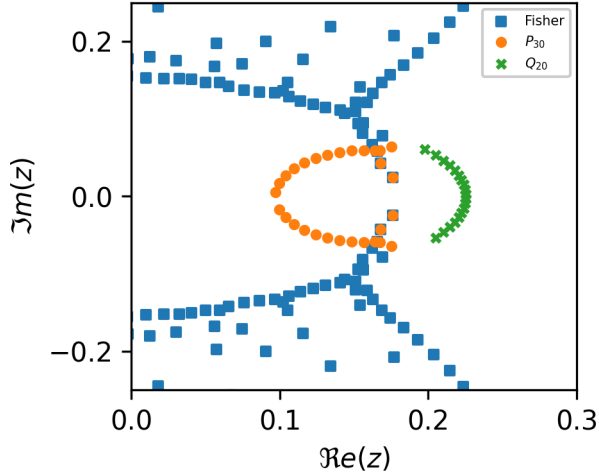


Figure 2: Fisher zeros from the shifted Padé approximation with $m = 30$, $n = 20$ and $z_0 = 0.17$. With only 30 terms in the approximation it was possible to identify the dominant zero.

as this value is sufficient to reproduce equivalent results.

8.4. Method Limitations in the XY Model

When applying zeros-based method to the XY model, fundamental differences emerge in comparison with the Ising case. Unlike the Ising model, the XY model does not exhibit a single well-defined dominant zero associated with the phase transition. Instead, the transition must be identified from the cuspd formed by the internal boundary of zeros, see Fig. 5, combined with a finite-size scaling analysis as discussed in Ref. [16].

As in the EPD and MGF formulations, the shifted Padé approach reconstructs only a localized portion of the zeros map, with the extent of this region determined by the number of coefficients retained in the approximation, see Fig. 6. While this localized reconstruction is sufficient to identify

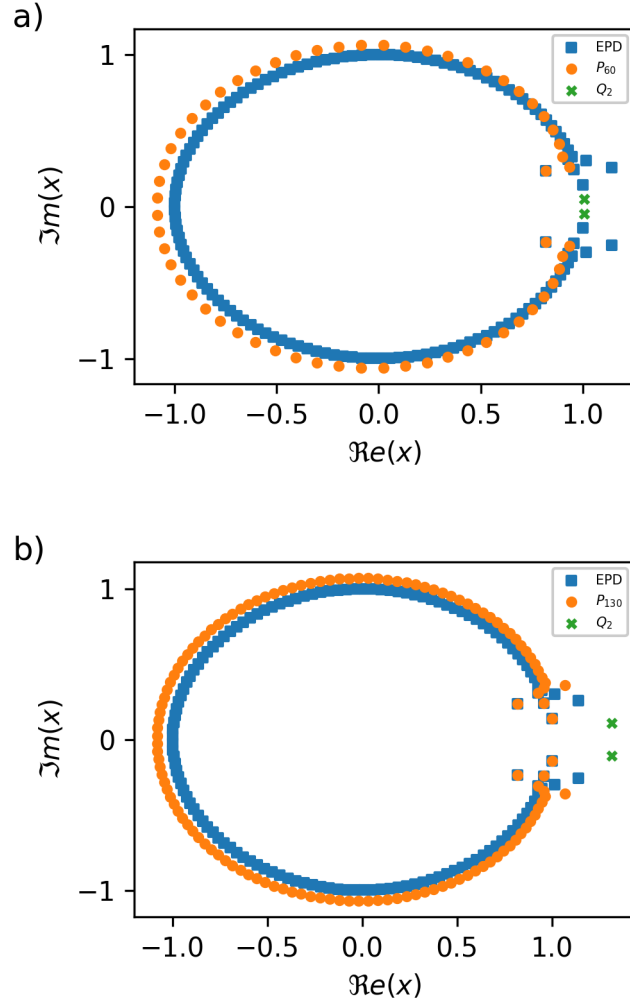


Figure 3: a) Distribution of EPD zeros from the Padé approximation with $m = 60$ and $n = 2$. In this case, the required polynomial order is nearly equal to the original EPD method, and a cluster of Q_2 zeros appears near the dominant zero, showing the necessity of a higher m value. b) Only for $m = 130$ the dominant zero is correctly estimated.

the vicinity of the cusp, it does not, by itself, allow for an unambiguous determination of the cusp position, since the global reference structure of the

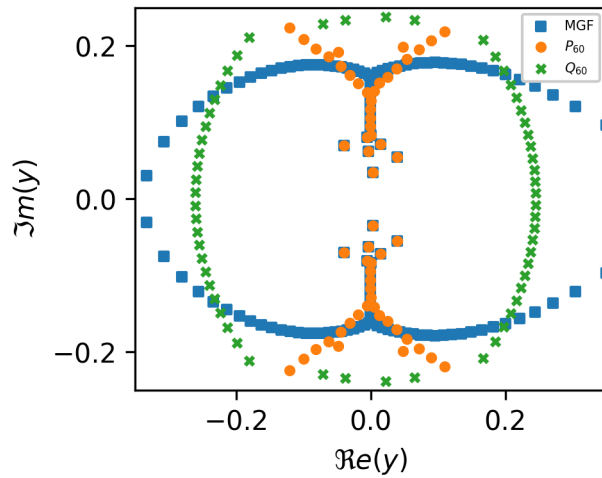


Figure 4: Padé approximation applied to the MGF method using $m = 60$ and $n = 60$, corresponding to half the polynomial degree of the original formulation.

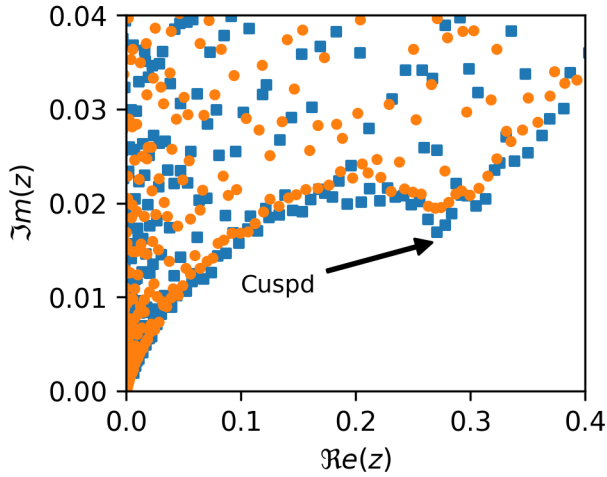


Figure 5: Two samples of Fisher zeros for the XY model with lattice size $L = 50$. The phase transition is identified from the cusp structure formed by the zeros in the complex plane. Notably, the cusp is not always sharply defined.

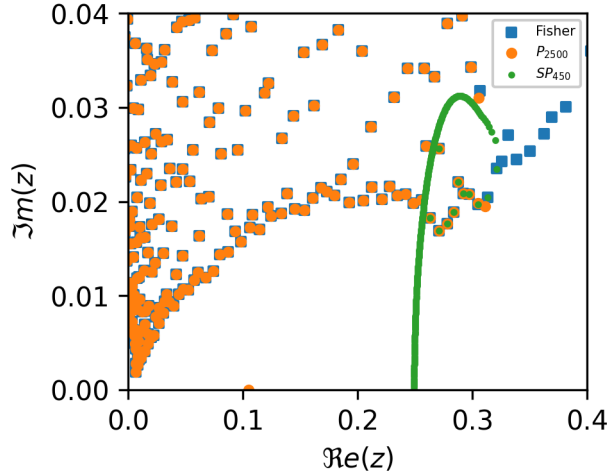


Figure 6: Zeros map for the Fisher, Padé, and shifted Padé (SPadé) approximations, with the shift taken at $z_0 = 0.27$. Note that the shifted Padé approximation captures only the region containing the cusp.

zeros map is lost, see the shifted Padé zeros plot alone without the Fisher zeros as reference in Fig. 7. The same problem is observed in the MGF and in the EPD methods.

In addition to these issues, the EPD and MGF formulations suffer from further intrinsic limitations: their convergence algorithms fail in the XY model, thereby preventing a reliable identification of the phase transition, as discussed in [Appendix A](#).

Taken together, the limitations associated with the localized reconstruction of the zeros map and the convergence problems render the EPD, MGF, and shifted Padé approaches unsuitable for an accurate determination of the phase transition. By contrast, the Padé approximation applied to the Fisher zeros provides a robust alternative, enabling a substantial reduction in the

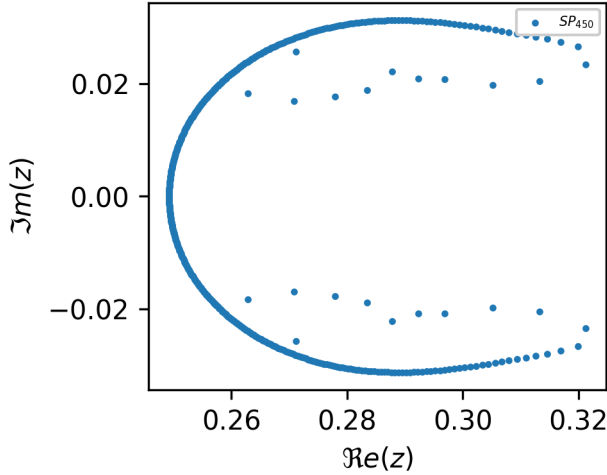


Figure 7: Zeros map for the shifted Padé approximation (SPadé), where the shift is taken at $z_0 = 0.27$. When only the shifted Padé zeros map is shown, it is not possible to precisely identify the location of the cusp.

number of required zeros while preserving the global cusp structure essential for identifying the transition, see Fig. 7.

Despite these limitations, and in order to enable a systematic comparison among the different methods, we apply the EPD, MGF, and shifted Padé approaches to the XY model. The Fisher zeros formulation is used as a reference throughout this comparison to guarantee a good evaluation, the analysis was carried as follows. In particular, the temperatures employed in the EPD and MGF analyses are chosen as the finite-size transition temperatures $T_{BKT}(L)$ obtained from the Fisher zeros. Similarly, the displacement parameter z_0 in the shifted Padé construction is set to the cusp position identified in the Fisher zeros map for a lattice of size $L = 50$. Furthermore, the zeros obtained from these methods are mapped onto the Fisher zeros plane, in a manner

similar to that shown in Fig. 6, and the analysis is carried out following the procedure described in Ref. [16]. This procedure ensures that the evaluation is performed in the vicinity of the cusp structure associated with the transition, thereby yielding accurate results. The finite-size scaling for the Fisher and the MGF zeros are shown in Fig. 8, the critical temperatures obtained with each method are discussed in the next section.

Despite these limitations, and in order to enable a systematic comparison among the different methods, we nonetheless apply the EPD, MGF, and shifted Padé approaches to the XY model. The Fisher zeros formulation is adopted as a reference to ensure a consistent and reliable evaluation. The analysis is conducted by setting the parameters of each method using information extracted from the Fisher zeros, thereby guaranteeing that all approaches probe the same critical region. Specifically, the temperatures employed in the EPD and MGF analyses are chosen as the finite-size transition temperatures $T_{\text{BKT}}(L)$ estimated from the Fisher zeros. Likewise, the displacement parameter z_0 in the shifted Padé construction is set to the cusp position identified in the Fisher zeros map for a lattice of size $L = 50$. Thereafter, the zeros obtained from the EPD, MGF, and shifted Padé methods are mapped onto the Fisher zeros plane in a manner similar to that shown in Fig. 6 and the analysis is carried out following the procedure described in Ref. [16]. This construction ensures that the analysis is performed in the vicinity of the cusp structure associated with the transition. The finite-size scaling of the Fisher and MGF zeros is shown in Fig. 8, and the critical temperatures extracted using each method are discussed in the next section.

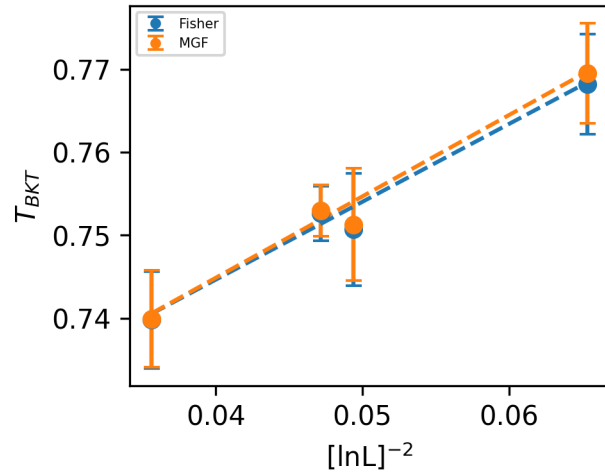


Figure 8: Finite-size scaling for the XY model as a function of $[\ln L]^{-2}$ [26], using system sizes $L = [50, 90, 100, 200]$. For clarity, only the linear regressions obtained from the Fisher and MGF zeros are shown. The regression lines corresponding to the other methods coincide exactly with one of these two and therefore lie directly on top of them. Table 1 summarizes the numerical values of T_c for each method.

8.5. Critical Temperature and Number of Zeros

Table 1 summarizes the critical temperature estimates obtained using the different methods considered in this work. As discussed before, the shifted Padé approximation cannot be combined with the convergence algorithms of the EPD and MGF zeros; therefore, results for these cases are not reported. In addition, for the EPD formulation, the Padé approximation does not lead to any improvement over the standard approach (see Sec. 8.2) and is thus omitted. Overall, the estimates are consistent across all approaches and in good agreement with the exact and previously reported values in the literature.

Critical Temperature		
Method	Ising	XY
Fisher	2.27098(8)	0.707(7)
Padé–Fisher	2.27098(8)	0.707(7)
SPadé–Fisher	2.27098(8)	0.707(7)
EPD	2.27098(8)	0.707(7)
MGF	2.26799(5)	0.705(7)
Padé–MGF	2.26799(5)	0.705(7)

Table 1: Critical temperature found for the Ising model and XY model for each method. For the Ising model the exact critical temperature is $T_c = 2.269185$. For the XY model, literature estimates of the transition temperature are approximately 0.700 [27, 16, 11].

The reduction in polynomial degree and, consequently, in the number of zeros is illustrated in Tables 2 for the Ising and XY models. For the Ising

model with $L = 150$, the Padé approximation reduces the number of Fisher zeros from 22,500 to 5,000, while in the MGF formulation the number of zeros is reduced by half. As a direct consequence, the computational cost of finding the polynomial roots using MPSolve [28, 29] decreases dramatically: for instance, in the $L = 150$ Ising lattice, the complete Fisher zeros computation required about 34 minutes ¹, whereas the Padé method required only 80 seconds. The shifted Padé method further reduces the number of zeros to 150, with a total runtime of approximately 3 minutes.

A similar trend is observed in the XY model with $L = 200$, where the full Fisher zeros map required 3.46 hours of computation, while its Padé counterpart was completed in approximately 1 hour, and the shifted Padé version further decreased it to only 21 minutes.

These results demonstrate that the Padé approximation preserves the physical content of the original methods while significantly improving computational performance. The zeros obtained from the Padé based formulations coincide with those from the full polynomial, confirming that the approximation introduces no measurable deviation in the estimation of the critical temperature.

9. Closing Remarks

The analysis presented in this work demonstrates that the Padé approximation provides an efficient and accurate method for investigating phase transitions through partition function zeros. When applied to the Fisher

¹Time measured on a Dell Inspiron system (Intel i7-7700HQ, 16 GB RAM) using a Python implementation with the `mpmath` library for arbitrary precision arithmetic.

Ising Model				
Method	$L=24$	$L=32$	$L=64$	$L=150$
Fisher	576	1024	4096	22500
Padé–Fisher	150	1000	2500	5000
SPadé–Fisher	30	30	50	150
EPD	136	193	429	1687
MGF	120	120	120	120
Padé–MGF	60	60	60	60

XY Model				
Method	$L=50$	$L=90$	$L=100$	$L=200$
Fisher	4751	14580	18001	68000
Padé–Fisher	2500	7700	9500	36000
SPadé–Fisher	350	900	1000	1500
EPD	559	948	1089	2092
MGF	320	320	320	320
Padé–MGF	160	160	160	160

Table 2: Number of zeros required to determine the critical temperature for the Ising model and XY model. The number of zeros increases with system size L for the EPD and Fisher related methods, whereas for the MGF related methods it remains constant.

and MGF formulations, the Padé method preserves the physical content of the original approaches while significantly reducing the polynomial degree

and, consequently, the number of zeros required to identify the dominant root. This reduction translates directly into a substantial decrease in computational cost without any loss of numerical precision. In contrast, its application to the EPD zeros does not offer any improvement, as the polynomial order required to find the dominant zero is similar in both methods.

The method was validated using the two-dimensional Ising and **anisotropic Heisenberg** (XY) models , demonstrating agreement with the critical temperature values reported in the literature while reducing the number of zeros required. For the largest Ising lattice studied, the Padé-Fisher approach reduced the number of zeros from 25,000 to 5,000, decreasing the computation time for locating the dominant zero from 34 minutes to 80 seconds. In the XY model, the number of Fisher zeros decreased from 68,000 to 36,000, with the computation time reduced from 3.46 hours to approximately one hour. The shifted Padé variant further reduces the number of zeros by restricting the analysis to a localized region of the zeros map, requiring only 150 zeros for the Ising model and approximately 1,000 for the XY model, with corresponding runtimes of approximately 3 minutes and 21 minutes, respectively.

Although all methods considered yield accurate estimates of the critical temperature in systems with a well-defined dominant zero, the EPD, MGF, and shifted Padé approaches are not suitable for a direct analysis of the XY model. The EPD and MGF formulations fail to reliably identify the phase transition due to fundamental limitations of their convergence algorithms. Furthermore, like the shifted Padé approximation, these methods reconstruct only a restricted region of the zeros map and therefore cannot capture its global structure, leading to the loss of the cusp information that characterizes

the XY transition. In contrast, the combined use of Fisher zeros and the Padé approximation provides a robust and reliable approach for analyzing the XY model, preserving the essential features of the zeros distribution.

Data Availability

The raw data used in the XY model can be found in Zenodo [25].

Acknowledgements

This study was financed by the São Paulo Research Foundation (FAPESP), Brasil. Process Number 2023/15458-4.

Appendix A. Non-Convergent Behavior of Zeros in the XY Model

Additional challenges arise when applying the EPD or MGF zero-based methods to the XY model. In contrast to the Ising case, see Fig. A.9, where a well-defined dominant zero is observed, the XY model exhibits an extended line of zeros in the region where a single dominant zero would normally be expected, even for temperature far from the critical point, see Fig. A.10. As a consequence of the continuous line of zeros for the XY model, the convergence algorithms discussed in this work tend to approach temperatures close to any initial value β_0 leading to a wrong estimation of $T_{BKT}(L)$. It should be noted that convergence is observed for small lattice sizes, yielding estimates consistent with the expected critical temperature. However, this behavior does not persist for larger systems.

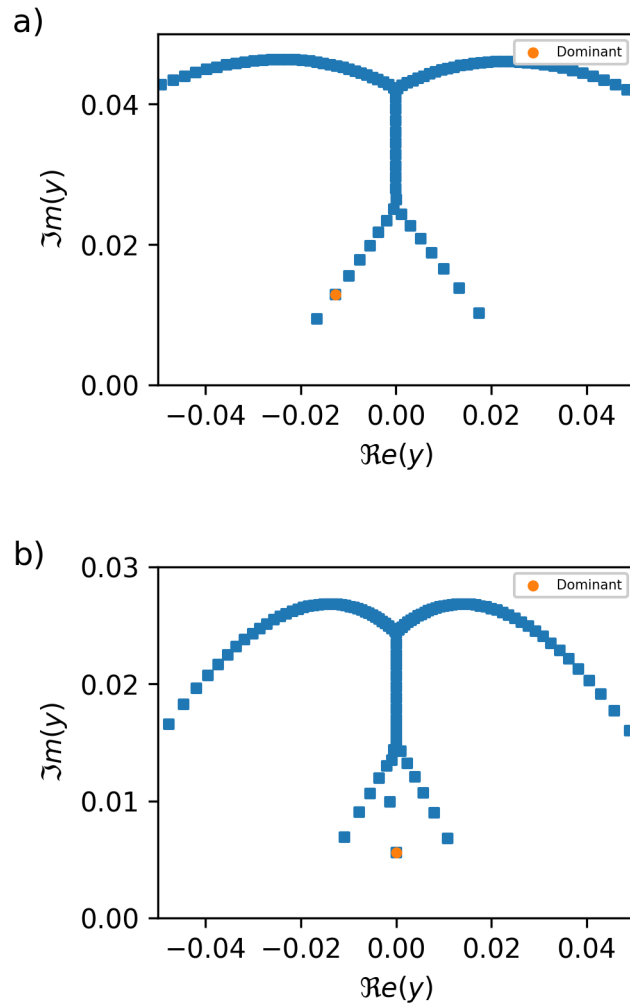


Figure A.9: MGF zeros for the Ising model with lattice size $L = 150$ at (a) $T = 3.0$ and (b) $T_c = 2.265$. At the critical temperature, the dominant zero is clearly identifiable.

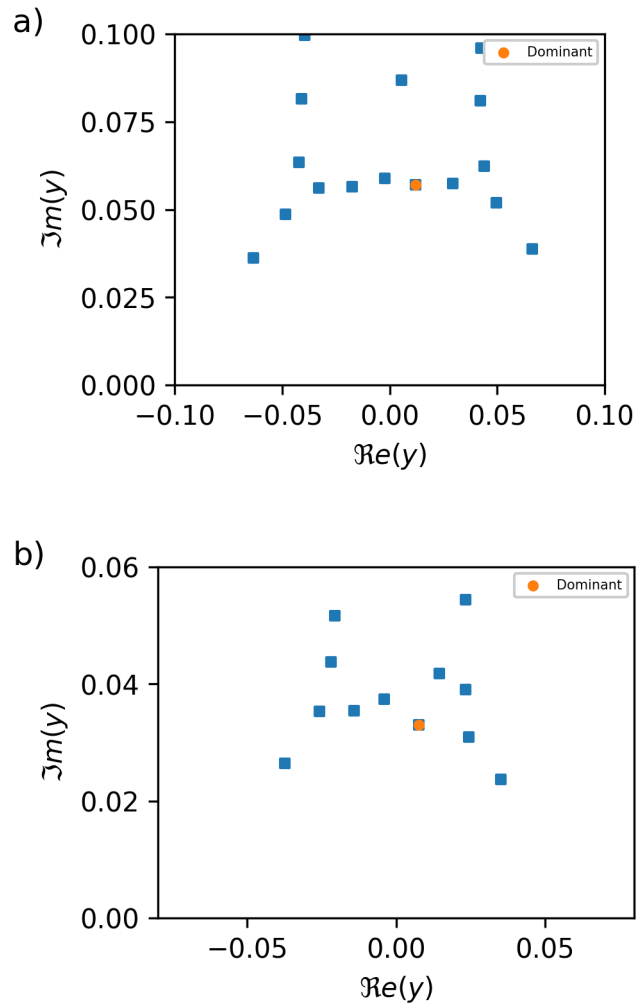


Figure A.10: MGF zeros for the XY model with lattice size $L = 100$ at (a) $T = 2.0$ and (b) $T_{\text{BKT}} = 0.7587$. In contrast to the Ising case, the zeros do not exhibit a distinct dominant zero; instead, several zeros appear near $(0,0)$, which may be incorrectly identified as dominant by the convergence algorithm.

Appendix B. Computational Challenges in Shifted Padé Coefficient Construction

To apply the Shifted Padé method to the Fisher zeros it is necessary to calculate the coefficients given by,

$$c_k = \sum_{n=k}^N g(E_n) \binom{n}{k} z_0^{n-k}, \quad k = 0, 1, \dots, N, \quad (\text{B.1})$$

where $g(E_n)$ denotes the density of states and z_0 is the expansion point. This computation presents two main challenges. First, numerical instability may arise from overflow or underflow during the evaluation of the terms $g(E_n) \binom{n}{k} z_0^{n-k}$, since the combinatorial factor and the density of states can attain extremely large values, while z_0^{n-k} may become very small for values between 0 and 1. Second, the direct evaluation of the summation is computationally expensive since N can be large and there is a binomial coefficient that must be computed. Therefore, this shifts the computational cost from the root finding algorithm to the coefficient construction itself.

Although the results presented in this work were obtained using Python and the `mpmath` library for arbitrary-precision arithmetic, the shifted Padé approximation required a more efficient implementation. To achieve competitive computational performance, the shifted Padé algorithm was implemented in Fortran using Horner's method in combination with the arbitrary-precision MPFUN library [30]. An OpenMP-parallelized version was also explored. However, for the largest XY lattice considered, it yielded only a modest performance gain of approximately 15%.

References

- [1] C. N. Yang, T. D. Lee, Statistical theory of equations of state and phase transitions. i. theory of condensation, *Phys. Rev.* 87 (1952) 404–409. [doi:10.1103/PhysRev.87.404](https://doi.org/10.1103/PhysRev.87.404).
URL <https://link.aps.org/doi/10.1103/PhysRev.87.404>
- [2] T. D. Lee, C. N. Yang, Statistical theory of equations of state and phase transitions. ii. lattice gas and ising model, *Phys. Rev.* 87 (1952) 410–419. [doi:10.1103/PhysRev.87.410](https://doi.org/10.1103/PhysRev.87.410).
URL <https://link.aps.org/doi/10.1103/PhysRev.87.410>
- [3] J. C. Rocha, S. Schnabel, D. P. Landau, M. Bachmann, Leading fisher partition function zeros as indicators of structural transitions in macromolecules, *Physics Procedia* 57 (2014) 94–98, proceedings of the 27th Workshop on Computer Simulation Studies in Condensed Matter Physics (CSP2014). [doi:<https://doi.org/10.1016/j.phpro.2014.08.139>](https://doi.org/10.1016/j.phpro.2014.08.139).
URL <https://www.sciencedirect.com/science/article/pii/S1875389214002843>
- [4] M. Heyl, A. Polkovnikov, S. Kehrein, Dynamical quantum phase transitions in the transverse-field ising model, *Phys. Rev. Lett.* 110 (2013) 135704. [doi:10.1103/PhysRevLett.110.135704](https://doi.org/10.1103/PhysRevLett.110.135704).
URL <https://link.aps.org/doi/10.1103/PhysRevLett.110.135704>
- [5] I. BENA, M. DROZ, A. LIPOWSKI, Statistical mechanics of equilib-

rium and nonequilibrium phase transitions: The yang–lee formalism, International Journal of Modern Physics B 19 (29) (2005) 4269–4329. [doi:10.1142/s0217979205032759](https://doi.org/10.1142/s0217979205032759).

URL <http://dx.doi.org/10.1142/S0217979205032759>

[6] M. Krasnytska, B. Berche, Y. Holovatch, R. Kenna, Partition function zeros for the ising model on complete graphs and on annealed scale-free networks, Journal of Physics A: Mathematical and Theoretical 49 (13) (2016) 135001. [doi:10.1088/1751-8113/49/13/135001](https://doi.org/10.1088/1751-8113/49/13/135001).

URL <https://doi.org/10.1088/1751-8113/49/13/135001>

[7] W. van Dijk, C. Lobo, A. MacDonald, R. K. Bhaduri, Fisher zeros of a unitary bose gas, Canadian Journal of Physics 93 (8) (2015) 830–835. [arXiv:https://doi.org/10.1139/cjp-2014-0585](https://doi.org/10.1139/cjp-2014-0585), [doi:10.1139/cjp-2014-0585](https://doi.org/10.1139/cjp-2014-0585).

URL <https://doi.org/10.1139/cjp-2014-0585>

[8] X. Peng, H. Zhou, B.-B. Wei, J. Cui, J. Du, R.-B. Liu, Experimental observation of lee-yang zeros, Phys. Rev. Lett. 114 (2015) 010601. [doi:10.1103/PhysRevLett.114.010601](https://doi.org/10.1103/PhysRevLett.114.010601).

URL <https://link.aps.org/doi/10.1103/PhysRevLett.114.010601>

[9] A. Krishnan, M. Schmitt, R. Moessner, M. Heyl, Measuring complex-partition-function zeros of ising models in quantum simulators, Phys. Rev. A 100 (2019) 022125. [doi:10.1103/PhysRevA.100.022125](https://doi.org/10.1103/PhysRevA.100.022125).

URL <https://link.aps.org/doi/10.1103/PhysRevA.100.022125>

[10] M. E. Fisher, The nature of critical points, in: W. Brittin (Ed.), *Lectures in Theoretical Physics*, Vol. 7C, University of Colorado Press, Boulder, 1965, Ch. 1, pp. 1–159.

[11] B. Costa, L. Mól, J. Rocha, Energy probability distribution zeros: A route to study phase transitions, *Computer Physics Communications* 216 (2017) 77 – 83. [doi:
https://doi.org/10.1016/j.cpc.2017.03.003](https://doi.org/10.1016/j.cpc.2017.03.003).
URL <http://www.sciencedirect.com/science/article/pii/S0010465517300796>

[12] R. G. M. Rodrigues, B. V. Costa, L. A. S. Mól, Moment-generating function zeros in the study of phase transitions, *Phys. Rev. E* 104 (2021) 064103. [doi:10.1103/PhysRevE.104.064103](https://doi.org/10.1103/PhysRevE.104.064103).
URL <https://link.aps.org/doi/10.1103/PhysRevE.104.064103>

[13] A. Deger, F. Brange, C. Flindt, Lee-yang theory, high cumulants, and large-deviation statistics of the magnetization in the ising model, *Phys. Rev. B* 102 (2020) 174418. [doi:10.1103/PhysRevB.102.174418](https://doi.org/10.1103/PhysRevB.102.174418).
URL <https://link.aps.org/doi/10.1103/PhysRevB.102.174418>

[14] A. B. Lima, L. A. S. Mól, B. V. Costa, The Fully Frustrated XY Model Revisited: A New Universality Class, *Journal of Statistical Physics* 175 (5) (2019) 960–971. [doi:10.1007/s10955-019-02271-x](https://doi.org/10.1007/s10955-019-02271-x).
URL <http://link.springer.com/10.1007/s10955-019-02271-x>

[15] B. V. Costa, L. A. Mól, J. C. Rocha, A New Algorithm to Study the Critical Behavior of Topological Phase Transitions, *Brazilian Journal*

of Physics 49 (2) (2019) 271–276. [doi:10.1007/s13538-019-00636-x](https://doi.org/10.1007/s13538-019-00636-x).
URL <https://link.springer.com/article/10.1007/s13538-019-00636-x>

[16] J. Rocha, L. Mól, B. Costa, Using zeros of the canonical partition function map to detect signatures of a berezinskii–kosterlitz–thouless transition, Computer Physics Communications 209 (2016) 88 – 91. [doi:https://doi.org/10.1016/j.cpc.2016.08.016](https://doi.org/10.1016/j.cpc.2016.08.016).
URL <http://www.sciencedirect.com/science/article/pii/S0010465516302466>

[17] W. H. Press, S. A. Teukolsky, W. T. Vetterling, B. P. Flannery, Numerical Recipes 3rd Edition: The Art of Scientific Computing, 3rd Edition, Cambridge University Press, USA, 2007.

[18] P. D. Beale, Exact distribution of energies in the two-dimensional ising model, Phys. Rev. Lett. 76 (1996) 78–81. [doi:10.1103/PhysRevLett.76.78](https://doi.org/10.1103/PhysRevLett.76.78).
URL <https://link.aps.org/doi/10.1103/PhysRevLett.76.78>

[19] J. M. Kosterlitz, D. J. Thouless, Ordering, metastability and phase transitions in two-dimensional systems, Journal of Physics C: Solid State Physics 6 (7) (1973) 1181. [doi:10.1088/0022-3719/6/7/010](https://doi.org/10.1088/0022-3719/6/7/010).
URL <https://doi.org/10.1088/0022-3719/6/7/010>

[20] J. M. Kosterlitz, D. J. Thouless, Long range order and metastability in two dimensional solids and superfluids. (application of dislocation theory), Journal of Physics C: Solid State Physics 5 (11) (1972) L124.

[doi:10.1088/0022-3719/5/11/002](https://doi.org/10.1088/0022-3719/5/11/002).
URL <https://doi.org/10.1088/0022-3719/5/11/002>

[21] J. Jose, D. Thouless, [40 Years Of Berezinskii–kosterlitz–thouless Theory](#), World Scientific Publishing Company, 2013.
URL <https://books.google.com.br/books?id=OfC6CgAAQBAJ>

[22] N. D. Mermin, H. Wagner, [Absence of ferromagnetism or antiferromagnetism in one- or two-dimensional isotropic heisenberg models](#), Phys. Rev. Lett. 17 (1966) 1133–1136. [doi:10.1103/PhysRevLett.17.1133](https://doi.org/10.1103/PhysRevLett.17.1133).
URL <https://link.aps.org/doi/10.1103/PhysRevLett.17.1133>

[23] M. Hasenbusch, [The two-dimensional xy model at the transition temperature: a high-precision monte carlo study](#), Journal of Physics A: Mathematical and General 38 (26) (2005) 5869. [doi:10.1088/0305-4470/38/26/003](https://doi.org/10.1088/0305-4470/38/26/003).
URL <https://doi.org/10.1088/0305-4470/38/26/003>

[24] P. Olsson, [Monte carlo analysis of the two-dimensional xy model. ii. comparison with the kosterlitz renormalization-group equations](#), Phys. Rev. B 52 (1995) 4526–4535. [doi:10.1103/PhysRevB.52.4526](https://doi.org/10.1103/PhysRevB.52.4526).
URL <https://link.aps.org/doi/10.1103/PhysRevB.52.4526>

[25] J. C. Siqueira Rocha, L. Mól, B. V. Costa, [Entropy per energy for the xy model](#) (Jun. 2025). [doi:10.5281/zenodo.15614663](https://doi.org/10.5281/zenodo.15614663).
URL <https://doi.org/10.5281/zenodo.15614663>

[26] R. Kenna, A. Irving, [Logarithmic corrections to scaling in the two dimensional xy-model](#), Physics Letters B 351 (1) (1995) 273–278.

doi:[https://doi.org/10.1016/0370-2693\(95\)00316-D](https://doi.org/10.1016/0370-2693(95)00316-D).

URL <https://www.sciencedirect.com/science/article/pii/037026939500316D>

[27] H. G. Evertz, D. P. Landau, [Critical dynamics in the two-dimensional classical xy model: A spin-dynamics study](#), Phys. Rev. B 54 (1996) 12302–12317. doi:[10.1103/PhysRevB.54.12302](https://doi.org/10.1103/PhysRevB.54.12302).

URL <https://link.aps.org/doi/10.1103/PhysRevB.54.12302>

[28] D. A. Bini, G. Fiorentino, [Design, analysis, and implementation of a multiprecision polynomial rootfinder](#), Numerical Algorithms 23 (2) (2000) 127–173. doi:[10.1023/A:1019199917103](https://doi.org/10.1023/A:1019199917103).

URL <https://doi.org/10.1023/A:1019199917103>

[29] D. A. Bini, L. Robol, [Solving secular and polynomial equations: A multiprecision algorithm](#), Journal of Computational and Applied Mathematics 272 (2014) 276–292. doi:<https://doi.org/10.1016/j.cam.2013.04.037>.

URL <https://www.sciencedirect.com/science/article/pii/S037704271300232X>

[30] D. H. Bailey, [Mpfun2020: A thread-safe arbitrary precision package with special functions](#) (2020).

URL <https://www.davidhbailey.com/dhbsoftware/>